Gas Metal Arc Welding Sequence Effect on Residual Stress and Distortion by using Finite Element Analysis

Harika Prabandapu*, S.R.Somayajulu

Department of Mechanical and Engineering, VNRJIET Hyderabad, India.

harikaprabandapu@gmail.com*, somayajulu_sr@vnrvjiet.in

Abstract: It is a well-known fact that fusion welding is being extensively used in a wide spectrum of fabrication industries. In spite of its being a versatile joining process of materials of any thickness, it suffers from some serious setbacks which impair the life of weldments in service. Of utmost concern are the evolution of inevitable residual stresses and distortion in weldments which are the direct result of complex non-uniform thermal cycles experienced during fusion welding. Over the past few decades, finite element method has gained ground as a well-established method to numerically analyze welding related problems. Numerical simulation based on finite element modeling is used to study the influence of welding sequences on the distribution of residual stress and distortion generated when welding a flat-bar stiffener to a steel plate. The simulation consists of sequentially coupled thermal and structural analyses. In Transient thermal analysis, time-dependent temperature distribution is determined. Temperatures from thermal analysis are applied as loads in a structural analysis yielding the three-dimensional residual stress and distortion fields. The effect of four welding sequences on the magnitude of residual stress and distortion in the plate is investigated.

Keywords — Numerical Simulation, residual stresses and distortion, transient thermal analysis, thermal and structural analysis

I. INTRODUCTION

1.1 General Introduction

Welding is the most prominent process for joining large components into complex assemblies or structures. A necessary condition for welding is that the two or more surfaces to be joined must be brought into intimate contact. When fusion takes place, the joint is achieved by melting of two or more work piece materials in a localized region. In contrast, the solid-state joining processes rely on plastic deformation of the surface asperities along the contact surface representing the original weld interface or the impending weld joint.

Arc welding is the most commonly used process in almost all manufacturing sectors ranging from small to large size fabrication industries, to strategic sectors such as aerospace, ship building etc. This is due to the fact that arc welding process is considered to be the most versatile joining method to ensure structural integrity in the steel joints. It is capable of joining materials of all thicknesses. A welding power supply is used to create and maintain an electric arc between an electrode and the base material to melt metals at the welding point. In such welding processes the power supply could be AC or DC, the electrode could be consumable or non-consumable and a filler material may or may not be added. The most common types of arc welding are:

Shielded Metal Arc Welding (SMAW): A process that uses a coated consumable electrode to lay the weld. As the electrode melts, the (flux) coating disintegrates, giving off shielding gases that protect the weld area from atmospheric gases and provides molten slag which covers the filler metal as it travels from the electrode to the weld pool. Once part of the weld pool, the slag floats to the surface and protects the weld from contamination as it solidifies. Once hardened, the slag must be chipped away to reveal the finished weld.

Gas Metal Arc Welding (GMAW): A process in which a continuous and consumable wire electrode and a shielding gas (usually an argon and carbon dioxide mixture) are fed through a welding gun.

Gas Tungsten Arc Welding (GTAW): A process that uses a non-consumable tungsten electrode to produce the weld. The weld area is protected from atmospheric contamination by a shielding gas, and a filler metal that is fed manually is usually used.

1.2 Gas Metal Arc Welding

The gas metal arc welding (GMAW) process has become a popular method for joining components of steel structures

 DOI : 10.35291/2454-9150.2020.0162

and is the most common joining method used in the shipbuilding industry. Arc welding relies on intense local heating at a joint where a certain amount of the base metal is melted and fused with additional metal from the welding electrode. The intense local heating causes severe thermal gradients in the welded component and the uneven cooling that follows produces residual stresses and distortion. Distortions can be especially problematic in the block assembly method used in shipbuilding. Excessive distortion of welded components results in misalignment of parts and often requires costly remedial measures such as flame straightening and cold bending to reduce distortion to an acceptable level.

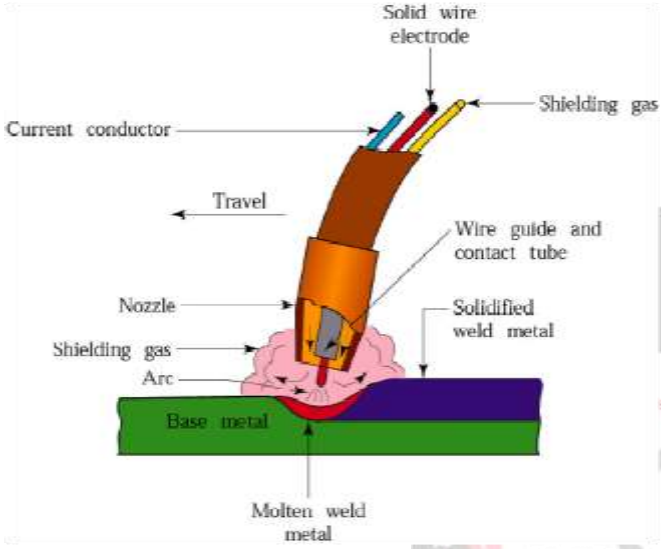

Fig1.2.1: Gas metal arc welding process

1.3 Design Recommendations for Weld Strength

Following are a few recommendations to improve the strength of the welded joint.

1. Square edged butt joint can be employed saving the edge preparation time if deep-penetration welding is used or the stock thickness is not great. Thicker stock or less penetrating methods may require grooved edges or groove welding.

2. For efficient and economical welding, minimize the stress that the joint must carry. Design the weld joint in such a fashion that it stays away from the stressed area or the part itself bears the load instead of the weld joints.

3. Groove welds should be designed to be in either compression or tension. Fillet welds should be in shear only. When using grooves for welds, follow the standard American Welding Society weld-groove dimensions.

4. Length of each fillet should be at least 4 times the fillet thickness when intermittent welds are used. If the joint is in compression, the spacing of the welds should not exceed 16 times the fillet thickness and for tension, the spacing may be as much as 32 times the fillet thickness.

1.4 Residual Stress and Distortion in Welding

The inherent local non-uniform heating and cooling cycles associated with the joining processes, in particular with the fusion welding processes, results in complex stresses and strains in and around the weld joint. These finally lead to the development of residual stress and distortion in welded structure. Residual stresses are referred to as internal stresses that would exist in a body after the removal of all external loads. Distortion refers to the permanent (*plastic*) strain that would be exhibited in terms of dimensional change after the welding is over. While the residual stresses can reduce the service life of a structure or even cause catastrophic failures, distortion usually results in misalignment with consequent difficulties in assembly and poor appearance of the final structure. Residual stress in weldments can have two major effects. It can produce distortion or cause premature failure, or both. Distortion is caused when the heated weld region contracts non uniformly, causing shrinkage in one part of a weld to exert eccentric forces on the weld cross section. The weldments strains elastically in response to this stress. Detectable distortion occurs as a result of this non uniform strain.

1.4.1 Residual Stress

Three main reasons for the development of residual stresses in welded structure are

1. Non-uniform heating and cooling of metal in and adjacent to the weld region,
2. Volume shrinkage of metal in weld during solidification (freezing), and
3. Microstructural change of metal, in particular solid state phase change in steel, on solidification leading to volumetric strain.
4. Residual stresses can occur through a variety of mechanisms including inelastic (plastic) deformations
5. Heat from welding may cause localized expansion, which is taken up during welding by either the molten metal or the placement of parts being welded.
6. When undesired residual stress is present from prior metalworking operations, the amount of residual stress may be reduced using several methods.

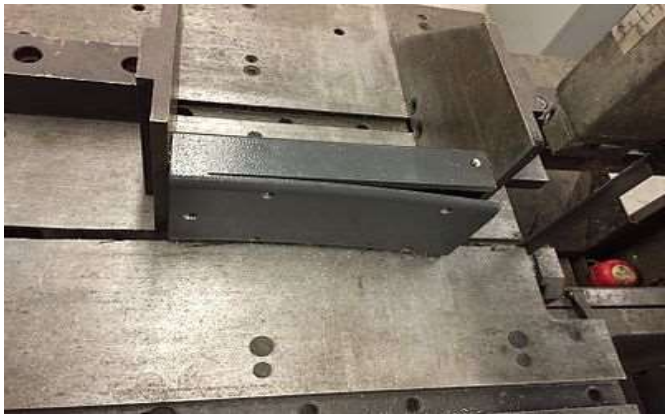

Fig1.4.1: Residual stress in a roll formed HSS tubing visible during band-saw slitting

 DOI : 10.35291/2454-9150.2020.0162

Typical changes in temperature and thermally induced stresses during welding are shown schematically in the Figure 1.4.2. The section A-A is far away from the welding heat source and thus, is not affected by the same. The welding heat source is along the section B-B. Thus, the longitudinal stresses will be close to zero in the region underneath the heat source since molten metal cannot withstand any stress. In the region slightly away from the melt pool in the transverse direction along section B-B, compressive stresses will be generated since thermal expansion of this region will be restrained by the surrounding colder material, which is at lower temperature. Along the section C-C, the weld metal and

the adjacent base metal are cooled and would shrink, thus producing tensile stresses since the compressive stresses due to shrinkage in solidified melt pool will be opposed by the surrounding colder material. As the weld metal will cool further, greater tensile stresses will be generated in the weld center and compressive in the base metal as apparent along the section D-D.

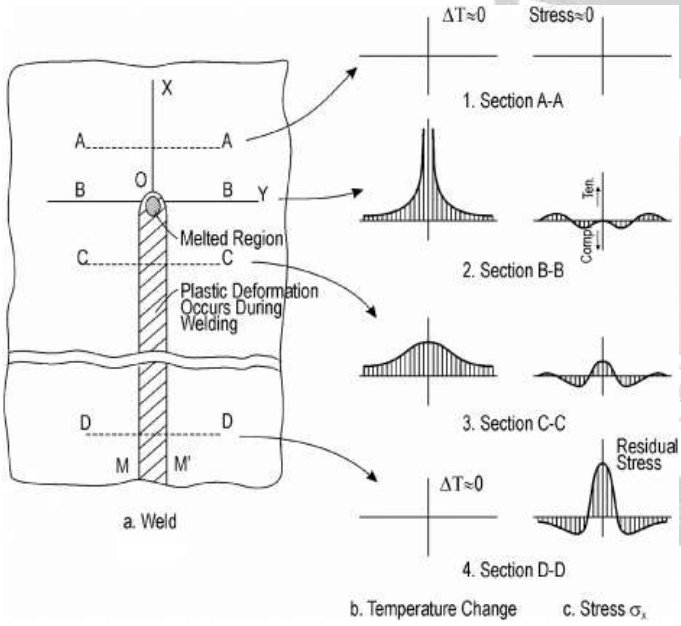

Fig. 1.4.2: Schematic distributions of temperature and longitudinal residual stresses in fusion welding

1.4.2 Effects of Residual Stress and Stress Relieving Methods

The effect of residual stress can be summarized as follows:

• The effect of weld induced residual stresses on the performance of a welded structure is significant only for the phenomena that occur at low applied stresses, such as brittle fracture, fatigue and stress corrosion cracking.

• As the level of applied stress increases, the effect of residual stress decreases.

• The effect of residual stress tends to decrease after repeated loading.

• The effect of residual stress on the performance of welded structures under applied stresses greater than the yield strength is negligible.

Due to very high thermal gradient during welding process, it is not possible to avoid the generation of residual stress. However, a number of stress-relieving methods are available and applied after the welding.

These stress-relieving methods include

(a) Vibratory stress relieving,

(b) Peening of weld area,

(c) Post-weld heat treatment etc.

Residual stress can also be minimized if proper measures are taken during welding, such as preheating to primarily reduce the temperature gradient and cooling rate, weld sequencing, preferring fillet weld over a butt weld, etc.

1.4.3 Welding Distortion

Welding distortion is caused by the non-uniform expansion and contraction of the weld metal and the adjacent base metal during the heating and cooling cycle of the welding process. The extent of welding distortion will depend on various factors such as:

(a) Geometry of the joint,

(b) Type of weld preparation,

(c) Width or volume of the web,

(d) Rate of heat input during welding process,

(e) Volume of weld deposition,

(f) Alignment of structural elements in the weldments, and

(g) The sequence in which welds are made.

Figure 2 schematically shows six types of welding distortion which common in fusion arc are welding –

(a) Transverse (b) Longitudinal,

(c) Angular (d) Rotational,

(e) Longitudinal bending (f) Buckling.

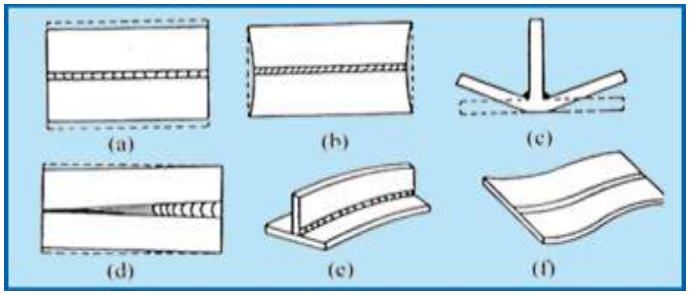

Fig. 1.4.3 Types of distortion in fusion welding

 DOI : 10.35291/2454-9150.2020.0162

Guidelines for Minimizing Distortion:

- Balance welds around the neutral axis — Welding on both sides of the plate offsets one shrinkage force with another, to minimize distortion.

- Heavier sections are less prone to distortion. So if distortion prevention is important to the application, designers should consider the use of thicker, more rigid components.
- Long and thin sections are readily distorted and buckled unless a good rigid support is provided. Use of short-flanged butt joint can minimize distortion in this case.
- Whenever possible, try to place welded joints in symmetric position. Distortion can be reduced by placing welds opposite to one another which balance the shrinkage force in the weld fillets.
- If sections of unequal thickness are to be welded together, then distortion can be reduced by machining a groove in the thicker section such that the thickness of the both part at the welded section becomes equal.
- When dimensioning welded assemblies, it is essential that consideration be given to the shrinkage inherent in each weld.
- **Intermittent welding** — to minimize the amount of weld metal, use intermittent welds instead of continuous welds where possible.
- **Place welds near the neutral axis, or the center of the part** — Distortion is reduced by providing less leverage for the shrinkage forces to pull the plates out of alignment.
- **Presetting the parts** — presetting parts before welding can make shrinkage work for you. The required amount of preset can be determined from a few trial welds.
- **Alternate the welding sequence** — A well-planned welding sequence involves placing weld metal at different points of the assembly so that, as the structure shrinks in one place, it counteracts the shrinkage forces of welds already made. An example of this is welding alternately on both sides of the neutral axis in making a complete joint penetration groove weld in a butt joint.
- **Thermal stress relieving** — another method for removing shrinkage forces is thermal stress relieving, i.e., controlled heating of the weldments to an elevated temperature, followed by controlled cooling.

II. LITERATURE SURVEY

2.1 Effect of welding sequence on residual stress in thin-walled octagonal pipe−plate structure

A three-dimensional finite element approach based on ABAQUS code was developed to investigate the effect of welding sequence on welding residual stress distribution in a thin-walled 6061 aluminum alloy structure is discussed in Ref. [1]. To obtain sound numerical results, in this study the thermo-mechanical behavior was simulated using a direct-coupled formulation. Nine different simulation sequences were carried out by single-pass TIG welding of an octagonal pipe−plate joint, and the distributions of longitudinal and transverse residual stresses both on the outer and inner surfaces of the pipe were analyzed.

2.2 Effect of welding Residual stress and Distortion on ship hull structural performance-

The finite element method is used to investigate the effects of welding-induced residual stress and distortion on the strength and behavior of ship hull structures is briefly discussed by Liam Gannon [2]. A finite element welding simulation consisting of sequentially coupled transient thermal and nonlinear structural analyses is used to predict the three-dimensional residual stress and distortion fields in welded stiffened plates. The strength and behavior of stiffened plates under axial load is characterized by normalized plots of average axial stress versus axial strain, commonly referred to as load-shortening curves. To conclude, a hull girder ultimate strength analysis is carried out using Smith's method with load-shortening curves generated by several different methods in this study [2]. Results indicate that welding-induced residual stress and distortion decrease the ultimate strength of flat-bar, angle, and tee-stiffened plates investigated in this study by as much as 17%, 15% and 13%, respectively.

2.3 Numerical Analysis of Effect of Process Parameters on Residual Stress in a Double Side TIG Welded Low Carbon Steel Plate

3D thermo-mechanical simulation model was developed to predict distribution of temperature and residual stresses during Tungsten Inert Gas (TIG) double-side arc welding (DSAW) process on a low carbon steel plate. Currents variations affect the total heat input per unit volume and directly influence the temperature distributions and consequently the residual stress profiles in the weld plate. 5. The speed variation of top and bottom torches causes preheating and post heating effects on the weld plate.

In this discussion two plates made of low carbon steel are welded together using double-torch double-sided TIG welding process without use of filler material. A parametric study on process variables such as welding current and welding speed were performed and its effects on residual stress were measured using FEM.

 DOI : 10.35291/2454-9150.2020.0162

2.4 Investigation of Arc Welding Variables Influenced by Temperature Cycle Developed in High Carbon Steel Welded Butt Joints and its Effect on Distortion.

The present work investigates the several welding variables developed due to transient temperature field during formation of butt joints by shielded metal arc (SMA) welding. Cars law -Jaeger's mathematical model has been utilized to portray the variation of thermal conductivity with experimental peak temperature by Jay deep Dutta [4]. To validate the temperature distribution experiment has been conducted for making butt joint of high carbon steel (AISI 1090). The cooling rate along the longitudinal direction from the fusion boundary has been derived by using Adam's two dimensional mathematical model. Effect of cooling rate is highlighted by results produced by Scanning Electron Microscope (SEM) images indicating the growth of crack. Distribution of surface heat flux has been estimated by implementation of Gaussian heat flux model. Effort has been made to correlate the distortion in welded structures due to highly variable thermal cycle with proper validation by implementation of temperature dependent transverse shrinkage model.

III. FINITE ELEMENT ANALYSIS

Since the majority of industrial components are made of metal, most FEA calculations involve metallic components. The analysis of metal components can be carried out by either linear or nonlinear stress analysis. Which analysis approach you use depends upon how far you want to push the design. Evaluating the effects of post-yield load cycling on the geometry, a nonlinear stress analysis should be carried out. In this case, the impact of strain hardening on the residual stresses and permanent set (deformation) is of most interest. Simulation uses the displacement formulation of the finite element method to calculate component displacements, strains, and stresses under internal and external loads. The geometry under analysis is discretized using tetrahedral (3D), triangular (2D), and beam elements, and solved by either a direct sparse or iterative solver.

3.1 Significance of Finite Element Simulation of Arc welding

The magnitude and distribution of welding-induced residual stress and distortion are affected by many factors including geometry, material properties and welding procedures. Although welding-induced residual stress and distortion may be measured experimentally using laser measuring devices, x-ray diffraction, neutron diffraction, these methods are time consuming and accuracy is often subject to the precision of the devices and measuring procedures. As an alternative to experimental methods, finite element analysis may be used to predict 3D residual stress and distortion fields produced by welding.

Until the emergence of high speed computer technology, analytical techniques were preferred to numerical methods for the analysis of welding due to the immense amount of calculation required to solve even the most basic problems using numerical methods. The use of numerical methods to analyze welding physics has seen rapid growth since the early 1970's when computer technology made possible the timely numerical solution of complicated problems. Numerical techniques have the advantage that they are able to predict the temperature field during welding and the associated residual stress and distortion without having to make many of the simplifying assumptions used in analytical solutions. The finite element method (FEM) is the most commonly used technique for this purpose. Using the FEM, heat transfer can be simulated accurately, allowing the transient temperature field associated with a moving heat source to be determined. This temperature field can subsequently be applied as a load in a structural analysis from which the associated stresses and deformations are determined.

2.2 Finite Element Modeling

Structural and thermal finite element analyses were performed using ANSYS to calculate residual stresses and distortions in a flat-bar stiffened plate resulting from welding the stiffener to the plate. The simulation consisted of two analyses. The first was a transient thermal analysis where the temperature distribution caused by a travelling heat source was determined. The second step consisted of a nonlinear structural analysis that was solved as a series of sequential load steps. Each load step represented an increment in the position of the heat source in the direction of welding. The temperatures from the thermal analysis associated with each load step were applied as loads in the structural analysis. This process was repeated multiple times until the welding was completed.

The plate and stiffener are both made from SM400A shipbuilding steel with a chemical composition given in Table 1. The plate is 150 mm x 150 mm with a thickness of 5 mm and the stiffener is 90 mm x 150 mm with a thickness of 5 mm. The stiffener is connected to the plate by 4 mm fillet welds deposited on both sides of the stiffener. The geometry of the stiffened plate is shown in Figure 3.1 and Figure 3.2 Four different welding sequences, shown in Figure 3.3, were investigated.

Table 1: Chemical composition of SM400A steel by wt%

Chemical composition (mass %)

C	Si	Mn	P	S
0.23	-	0.56	<0.035	<0.035

 DOI : 10.35291/2454-9150.2020.0162

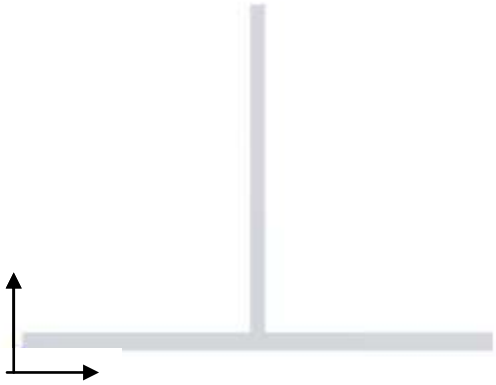

Fig. 3.1: Stiffened plate sectional view

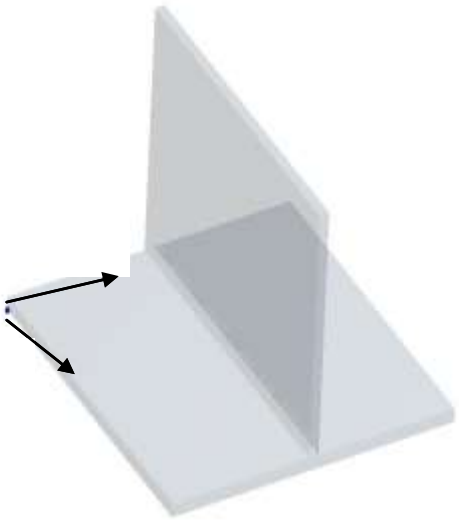

Fig. 3.2: Stiffened plate 3 dimensional view

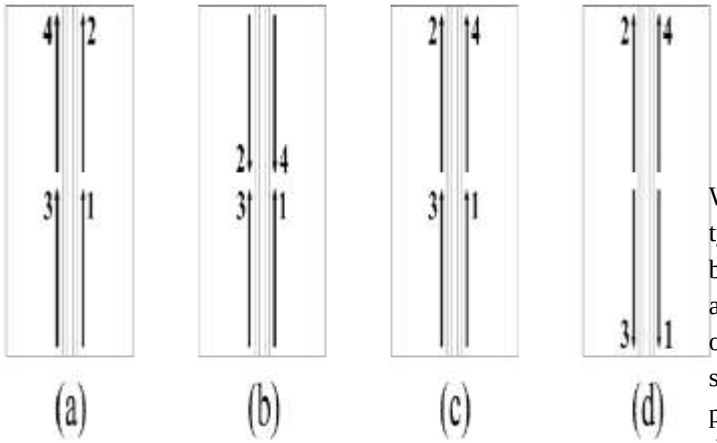

Fig. 3.3: Welding sequences

3.3 Commercial Finite Element solvers

Commercial finite element software's play an important role in solving many welding related problems. In early research works, finite element codes were written to compute transient thermal and stress fields in a weldment, using popular programming languages such as C, C++, and FORTRAN etc. While using these programming languages for writing finite element codes, certain difficulties are experienced by the researchers especially in the description of complex shapes and in post processing the results. With the advent of powerful CAD packages and meshing algorithms, popular general purpose standard finite element software's such as ABAQUS, ANSYS, MARC, NASTRAN etc. have been introduced and they are being increasingly used by the welding researchers for the past few decades.

ANSYS is the shortened term obtained from "System Analysis". It contains many bench mark tests drawn from a variety of resources such as NAFEMS (National Agency for Finite Element Methods and Standards), based in the United Kingdom, to validate the performance of elements under distorted or irregular shapes, different meshing schemes, different loading conditions, various solution algorithms, energy norms etc. ANSYS Mechanical software is a comprehensive **finite element analysis** (**FEA**) tool for structural analysis, including linear, nonlinear, dynamic, hydrodynamic and explicit studies. It provides a complete set of elements behavior, material models and equation solvers for a wide range of mechanical design problems.

Ansys, Inc. is an engineering simulation software (computer-aided engineering, or CAE) developer headquartered south of Pittsburgh in the South pointe business park in Cecil Township, Pennsylvania, and United States. One of its most significant products is Ansys CFD, a proprietary computational fluid dynamics (CFD) program.

ANSYS program is organized into different processors such as described below:

i. Preprocessor
ii. Solution Processor
iii. Post Processor and
iv. Time History post processor.

While the geometry of the weld joint specimen, element type, appropriate material properties, meshing patterns, boundary condition and load application can be dealt with at the preprocessor level, the type of solution (steady state or transient or modal or harmonic etc.), solver type, other solution options etc. can be specified at the solution processor. After obtaining solution of the model, the distributions of either temperature or heat fluxes or nodal displacements (distortions), principal strains or stresses in the model can be viewed in the postprocessor. The variation of any appropriate quantity of interest with time at a specified location in the model can be obtained in the time history post processor. ANSYS program has been used to compute the temperature distributions, temperature histories, thermal strains and residual stresses in weldments.

 DOI : 10.35291/2454-9150.2020.0162

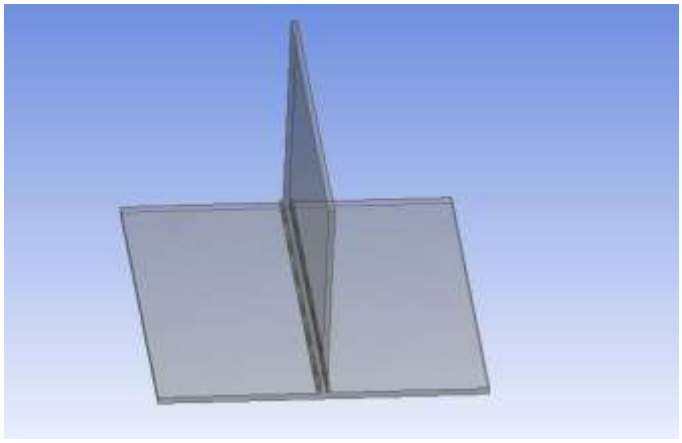

Fig. 3.4: Geometry modeled

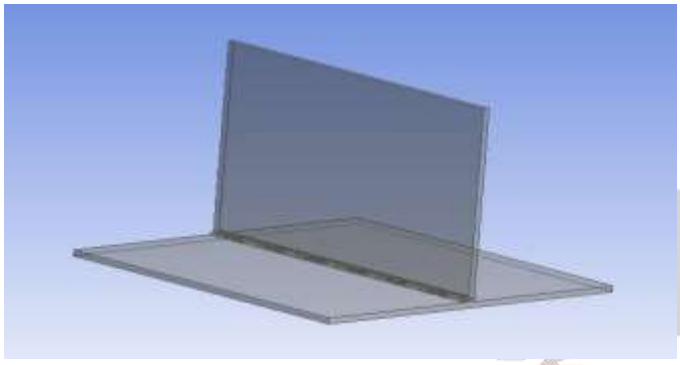

Fig. 3.4: Geometry modeled

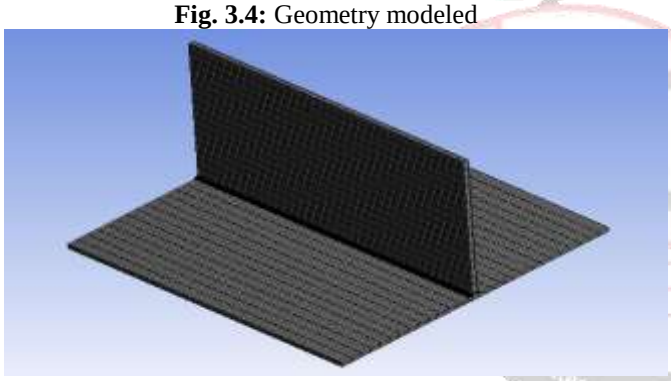

Fig. 3.4: Geometry modeled

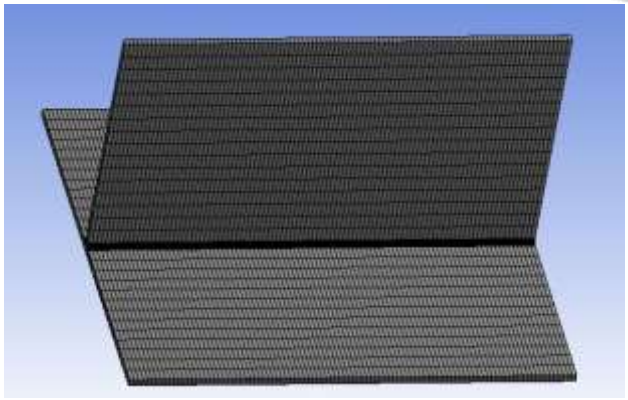

Fig. 3.5: Structured mesh of weld geometry

IV. THERMAL ANALYSIS

The main aim of transient thermal simulation is to capture the complex transient thermal cycles involved in arc welding of components. Fourier's law states that the rate of heat flow through a material is directly proportional to both the area of the section orthogonal to the direction of heat flow and to the temperature gradient in that direction. The heat equation, based on Fourier's law is derived here in one dimension, but can easily be extended to a more general three-dimensional case. Fourier's law for one-dimensional heat flow is expressed by:

$q(x, t) = -k\, dT/dx$

Where q(x, t) is heat flow, k is thermal conductivity and T is temperature.

As is needed for any finite element analysis, the governing differential equation is provided by Fourier law of heat conduction as below

$$\frac{\partial}{\partial x}\left(k_x \frac{\partial T}{\partial x}\right) + \frac{\partial}{\partial y}\left(k_y \frac{\partial T}{\partial y}\right) + \frac{\partial}{\partial z}\left(k_z \frac{\partial T}{\partial z}\right) + q = c\rho \frac{\partial T}{\partial t}$$

Where T is the temperature, kx, ky and kz are the thermal conductivities in x, y and z directions respectively, q is the internal heat generation, c is the specific heat capacity, ρ is the material density and t is the time.

The above equation can be easily derived on the basis of Fourier's law of heat conduction and the law of energy conservation. In order to formulate the problem of heat conduction in a solid body, the initial and boundary conditions need to be specified. The appropriate initial condition would be the initial temperature in the welding applications and is usually isothermal: $T(x, y, z, 0) = T_0$, where T_0 can be considered equal to the prevalent ambient temperature. The boundary conditions represent the law of interaction of the surfaces of the weld specimen with the ambience. The boundary conditions in welding are the convective (q_c) and radioactive (q_{rad}) heat flux losses from the surfaces of the welded plate given by:

$q_c = h\,(T - T_0)$

$q_{rad} = \varepsilon\, \sigma\, (T^4 - T_0^4)$

Where h is the convective heat transfer coefficient, T_0 is the ambient temperature, ε is the emissivity and σ is the Stefan-Boltzmann constant.

A Gaussian power distribution with an arc radius of 4.24 mm was assumed for the heat flux. The power distribution was defined relative to a coordinate system that was moving with the heat source as shown in Figure 8 and is expressed as:

$$q(\xi, y) = \frac{3Q}{\pi c^2} e^{-3\xi^2/c^2} e^{-3y^2/c^2}$$

Where c is the arc radius and Q is the heat input given by: $Q = \eta VI$

 DOI : 10.35291/2454-9150.2020.0162

Where, I is the current supplied, V is the voltage across the arc and η is the arc efficiency which is assumed to be 0.8 for CO_2 gas metal arc welding.

A summary of welding parameters is listed in Table 2.

Table 2: Welding conditions

Weld leg length (mm)	Current (A)	Voltage (V)	Welding speed (mm/min)
6	270	29	380

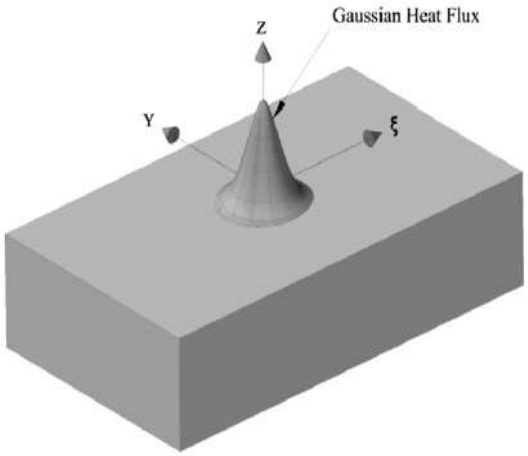

Fig. 4.1: Gaussian distributed heat source

The variation of thermal material properties such as thermal conductivity, density and specific heat with temperature are shown in Figure 9.

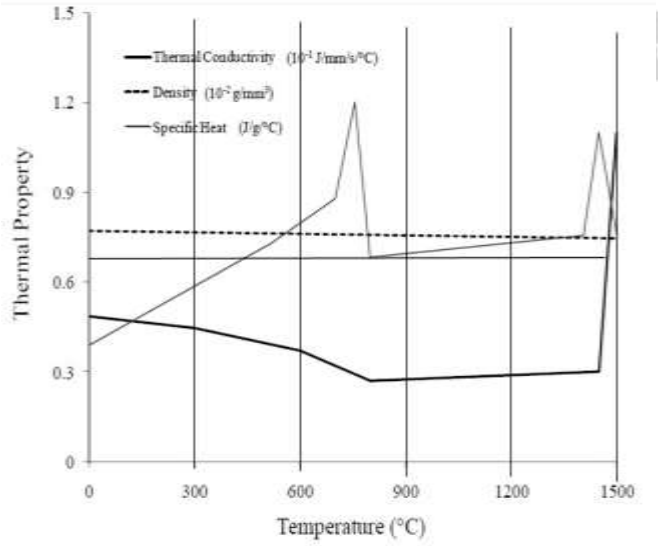

Fig. 4.2: Thermal material properties

Material properties play a significant role in welding simulation due to the fact that they have important effects on the accuracy of the results. The properties of the materials change when suffering from a thermal cycle, so the temperature-dependent physical properties and mechanical properties are considered in this work. Because of the lack of material data at elevated temperatures, the detailed material model for the material described is not available.

V. MECHANICAL ANALYSIS

The temperature history from the thermal analysis was used as a series of loads in the structural analysis, to solve for the unknown nodal displacements. Temperature histories obtained at various time steps in the previous thermal simulation, were given as inputs at the corresponding time steps to the structural model.

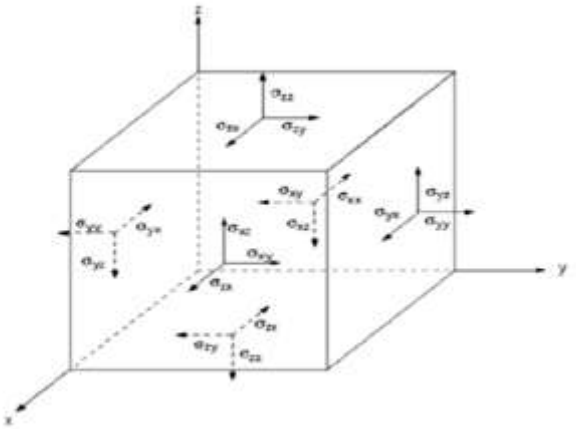

Fig: 5.1 3-dimensional stress-normal and shear stress components in tensor notation

The governing differential equations in terms of stresses for a three dimensional solid are:

$$\frac{\partial \sigma_x}{\partial x}+\frac{\partial \tau_{xy}}{\partial y}+\frac{\partial \tau_{xz}}{\partial z}+b_x=0$$

$$\frac{\partial \tau_{yx}}{\partial x}+\frac{\partial \sigma_y}{\partial y}+\frac{\partial \tau_{yz}}{\partial z}+b_y=0$$

$$\frac{\partial \tau_{zx}}{\partial x}+\frac{\partial \tau_{zy}}{\partial y}+\frac{\partial \sigma_z}{\partial z}+b_z=0$$

Where σ and τ are the normal and shear stress components and *bx*,… are body force components. These equations are multiplied by virtual displacements, integrated over the volume and added together to give the weighted residual, which using the Green-Gauss theorem can be written in terms of the principle of virtual displacements as follows

$$W=\iiint_V \delta\boldsymbol{\varepsilon}^T\boldsymbol{\sigma}dV-\iint_S \delta\boldsymbol{u}^T\boldsymbol{q}dS-\iiint_V \delta\boldsymbol{u}^T\boldsymbol{b}dV=0$$

 DOI : 10.35291/2454-9150.2020.0162

Where **σ** = (σx σy σz τxy τyz τzx) ^{T} are the normal and shear stress components, δ**ε** = (δεx δεy δεz δγxy δγyz δγzx) ^{T} and δ**u** = (δu δv δw) ^{T} are virtual strains and virtual displacements respectively, **q** = (qx qy qz)^{T} are applied surface loads and **b** = (bx by bz)^{T} are applied body forces. When the relationship between stresses and strains in above equation is nonlinear, the right hand side must be linearized using the directional derivative giving a system of algebraic equations of the form:

$K_T \Delta d = -r_I + r_q + r_b$

Where $\mathbf{k}_T$ is the tangent stiffness matrix, Δ**d** is the incremental displacement vector, **r**I is the internal force vector for the current solution and **r**q and **r**b are load vectors due to distributed loads and body forces respectively.

The modeling of the material behavior is a challenge as the deformation mechanisms vary widely in the large temperature range considered.

Temperature dependent mechanical material properties such as yield strength, elastic modulus, and thermal expansion coefficient and Poisson ratio are shown in Figure10

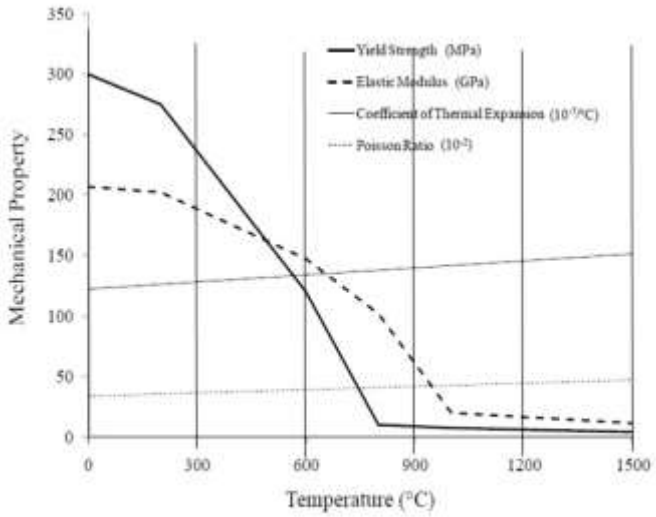

Fig. 5.2: Mechanical material properties

The welding process causes severe and visible deformations. Geometric nonlinearity arises when deformations are large enough to alter the distribution or orientation of applied loads, or the orientation of internal resisting forces and moments. Large deformations may

Deform a mesh so greatly that well-shaped elements become poorly shaped. Hence, the simulation should incorporate large deformation effects and strains. The large deformations and the use of small elements can cause these elements to be severely distorted. This problem can be overcome by the use of fine mesh and small time steps. It is assumed that the deformation can be decomposed into a number of components. The increments in total strain are computed from the incremental displacements during a non-linear finite element analysis. The elastic part of the strain gives the stresses, and there are a number of inelastic strain components that can be accounted for. The inelastic components of the total strain rate are the plastic strain rate, the viscos plastic strain rate, the creep strain rate, the thermal strain rate consisting of thermal expansion and volume changes due to phase transformations and the transformation plasticity strain rate. A welding simulation must at least account for elastic strains, thermal strains and one more inelastic strain component in order to give residual stresses. The mechanical analysis requires much more time due to more unknowns per node than in the thermal analysis. Furthermore, it is much more non-linear due to the mechanical material behavior.

VI. RESULTS AND DISCUSSION

By finite element analysis, welding simulation is carried out for four welding sequences of GMAW (Gas metal arc welding) and the effect on the residual stress and distortion are presented in this section. The longitudinal and transverse residual stresses; and the distortions occurred due to the welding sequences were presented and discussed.

6.1 Temperature distributions

Transient thermal numerical simulation is carried out for four welding sequence and temperature contour in (°C) at 6th second is shown in Figure 6.1.

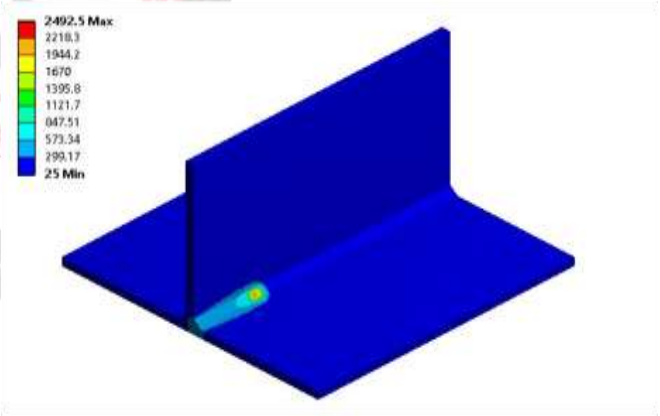

Sequence A

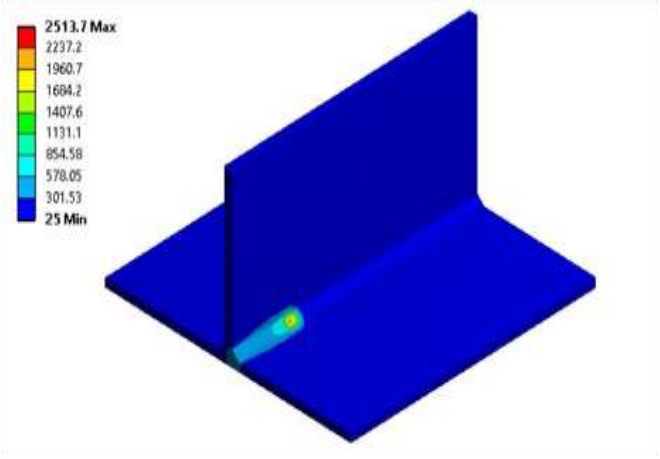

Sequence B

 DOI : 10.35291/2454-9150.2020.0162

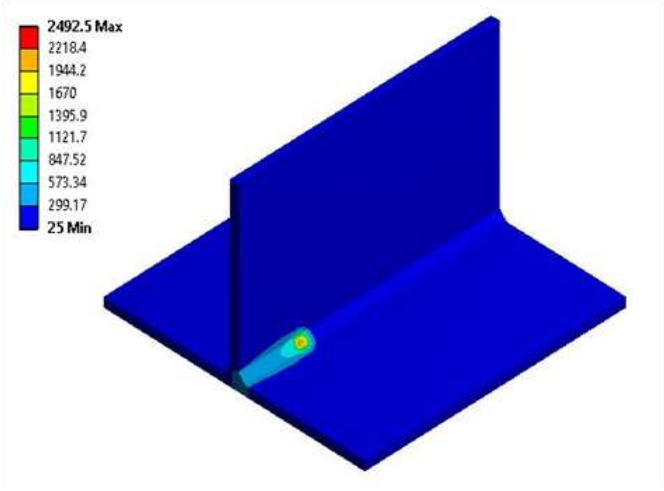

Sequence C

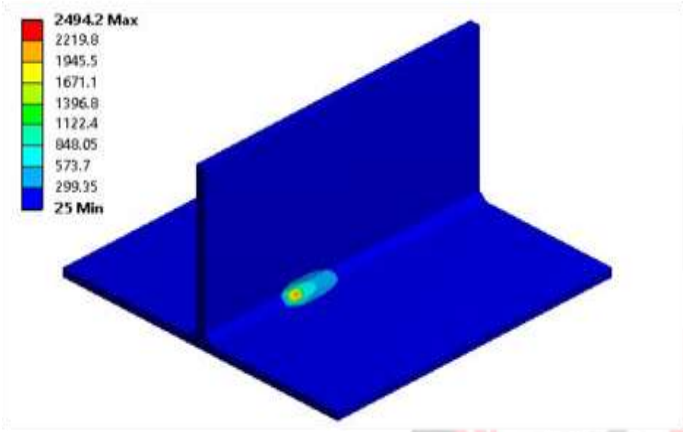

Sequence D

Fig. 6.1: Temperature contours

It is observed that temperature distributions around the source are typical of the fusion zone (FZ) and the heat affected zone (HAZ). It is also noticed that the heat source preheats a small region of weld plate ahead of the moving heat source. The peak temperature at the center of fusion zone is in proportion to the heat input. The heat generated by the moving heat source along the weld is gradually propagated towards all directions in the plate through conduction, convection and radiation.

The peak temperature achieved for each welding sequence is summarized in Table 3. Peak temperature is high for welding sequence B, low for welding sequence A and C.

Table 3: Peak temperature achieved for each welding sequence

Welding sequence	Peak temperature achieved (°C)
A	2492.5
B	2513.7
C	2492.5
D	2494.2

Figure 13 shows the first 100 s of the temperature time-history for welding sequence A at points A, B, C and D located as shown in Figure 6.3. Similarly for welding sequence B, C and D temperature time-history is shown in Figure 6.4, Figure 6.5 and Figure 6.6 respectively.

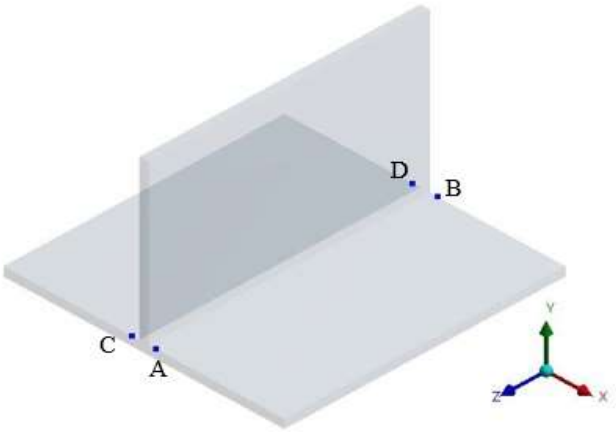

Fig. 6.2: Location for temperature time histories

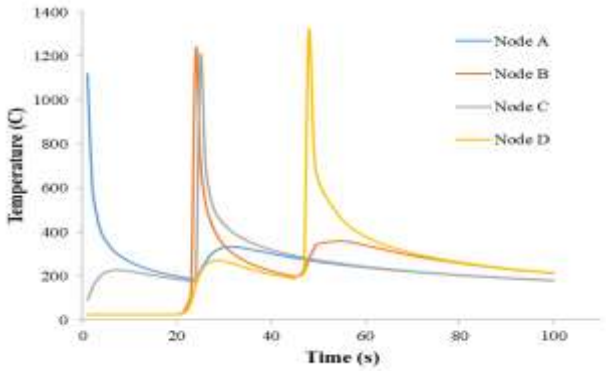

Fig.6.3: Temperature histories at point A, B, C and D for welding sequence A

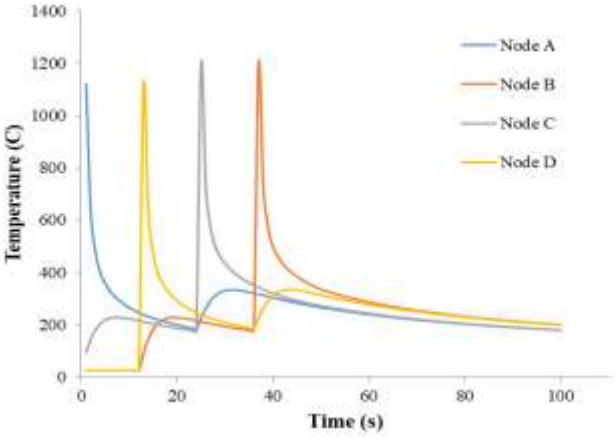

Fig.6.4: Temperature histories at point A, B, C and D for welding sequence B

 DOI : 10.35291/2454-9150.2020.0162

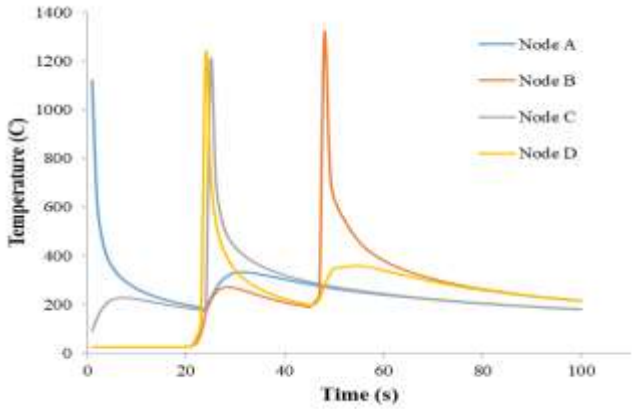

Fig. 6.5: Temperature histories at point A, B, C and D for welding sequence C

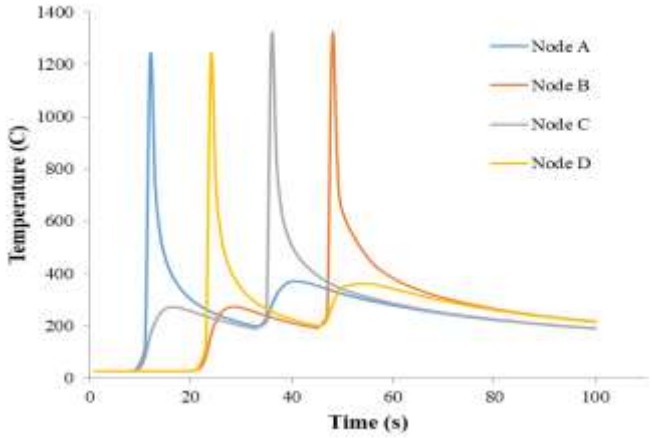

Fig. 6.6: Temperature histories at point A, B, C and D for welding sequence D

6.2 Residual stress distributions

Although residual stresses caused by welding are three-dimensional, the longitudinal and transverse component of residual stresses is considered to have the greatest influence on the strength of stiffened plates. It is evident that tensile residual stresses are resulted in the weld zones, which are balanced by the compressive residual stresses at the opposite sides. It is also obvious that the tensile residual stress zone is enlarged in accordance with the increase in the HAZ at higher heat input.

Figure 6.7 shows the simulated longitudinal residual stress distribution for four welding sequence at Z=0.15 m. For sequence A, maximum tensile longitudinal residual stress is 71.13 MPa and maximum compressive longitudinal residual stress is 27.54 MPa. For sequence B, maximum tensile longitudinal residual stress is 73.87 MPa and maximum compressive longitudinal residual stress is 27.39 MPa. For sequence C, maximum tensile longitudinal residual stress is 71.87 MPa and maximum compressive longitudinal residual stress is 28.20 MPa. For these three sequences maximum tensile and compressive longitudinal residual stress occurs at X=0.078 m at X=0.094 m respectively.

At these locations for sequence D, longitudinal residual stresses are 32.5 MPa and 7 MPa tensile. For sequence D, maximum tensile longitudinal residual stress is 110 MPa that is around 1.5 times higher than other sequences at X=0.083 m and maximum compressive longitudinal residual stress is 7.80 MPa that is 72% less than induced by other three sequences at X=0.11 m.

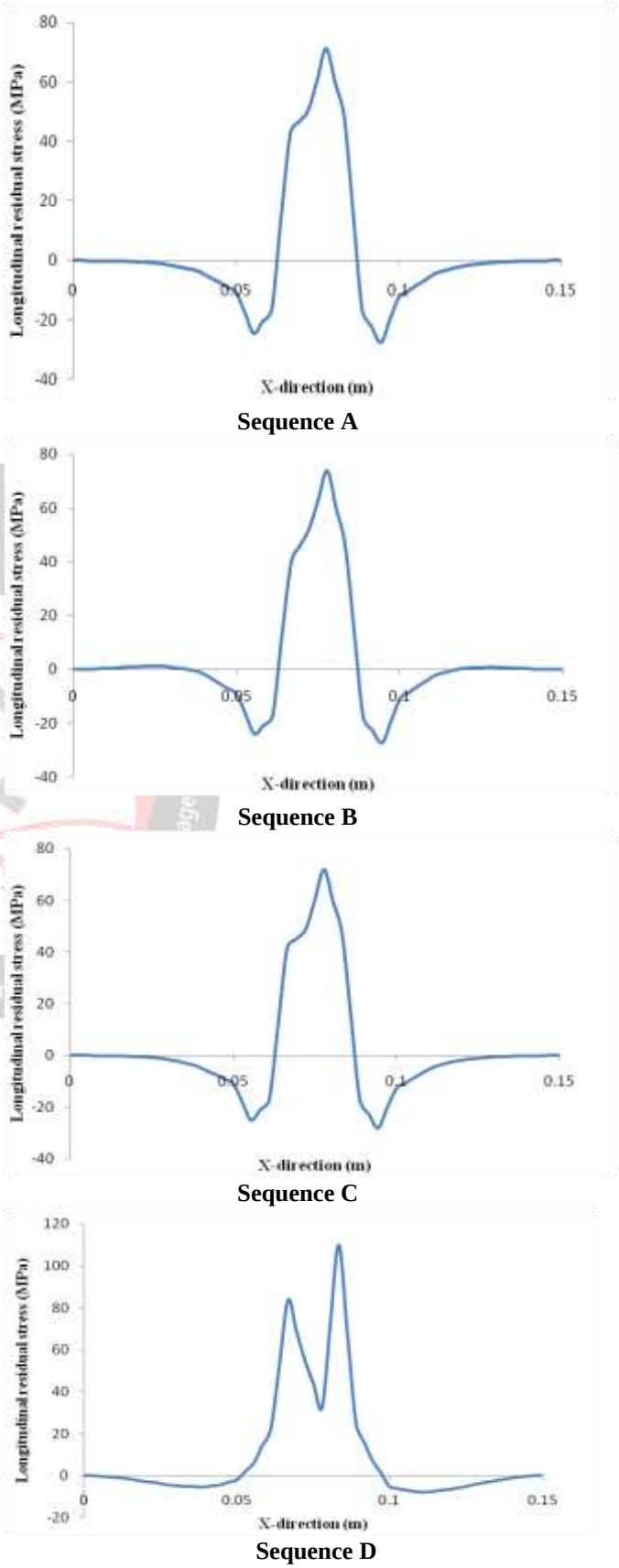

Fig. 6.7: Longitudinal residual stress distribution for welding sequences

 DOI : 10.35291/2454-9150.2020.0162

It is evident from the figure that the tensile stresses were developed in the weld zone. These tensile residual stresses gradually decrease in the transverse direction away from weld center line and become compressive residual stresses towards the edge of the plate. This is because during the cooling phase when the temperature of the weld zone falls rapidly, the weld metal tends to contract. This contraction of the weld metal is constrained by neighborhood of the weld zone, resulting in the tensile residual stresses in the weld zone. Compressive residual stresses were resulted in order to balance the tensile residual stresses for the equilibrium of the T-joint.

Transverse residual stresses distributions along weld line are typically compressive part in the ends of plate, otherwise are tensile part with magnitude of stresses is lower than longitudinal residual stress. Figure 6.8 shows the simulated transverse residual stress distribution for four welding sequence at Z=0.15 m. For sequence A, maximum tensile transverse residual stress is 42.7 MPa and maximum compressive transverse residual stress is 82.8 MPa. For sequence B, maximum tensile transverse residual stress is 37.4 MPa and maximum compressive transverse residual stress is 94 MPa. For sequence C, maximum tensile transverse residual stress is 42.4 MPa and maximum compressive transverse residual stress is 84.6 MPa. For these three sequences maximum tensile and compressive transverse residual stress occurs at X=0.067 m at X=0.15m respectively.

For sequence D, only compressive transverse stress is induced and it is maximum 205 MPa at X=0.078 m. notably, this sequence had less compressive longitudinal stress than other sequences.

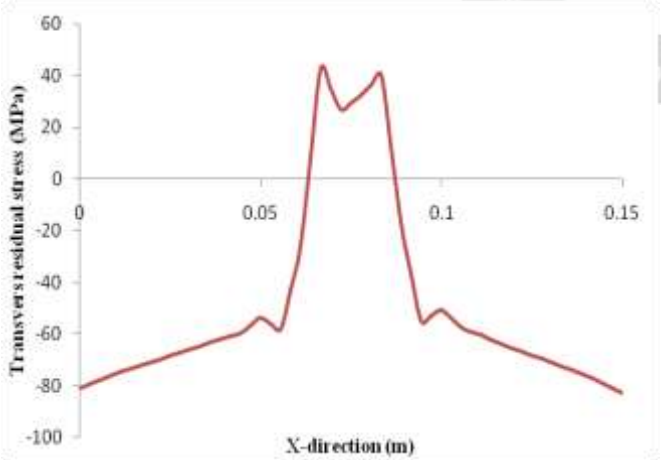

Sequence A

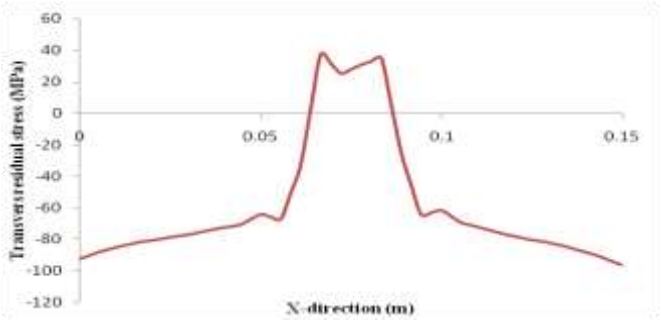

Sequence B

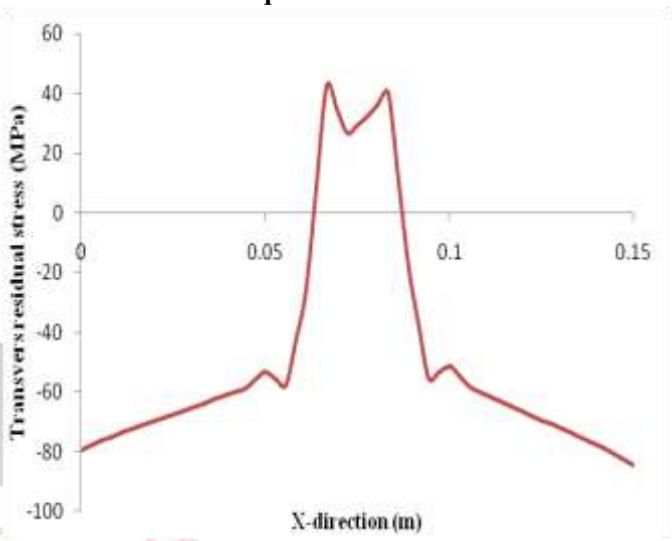

Sequence C

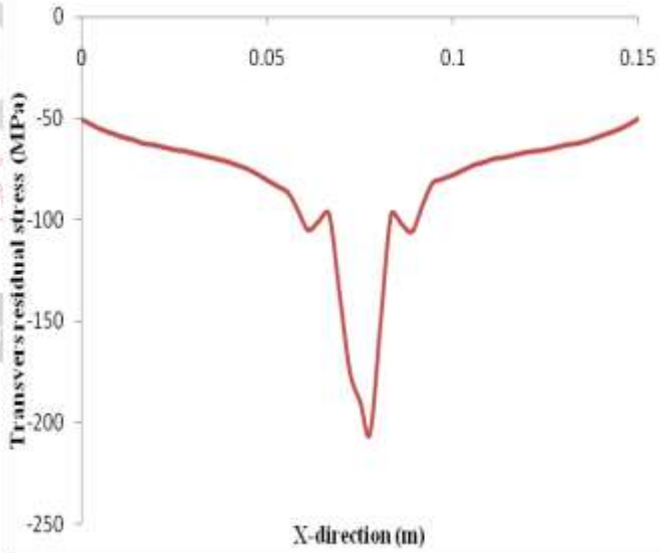

Sequence D

Fig. 6.8: Transverse residual stress distribution for welding sequences

To compare four welding sequences, maximum values of longitudinal and transverse residual stresses as well as von misses stress for each welding sequence were summarized in Table 4

.

Table 4: Maximum longitudinal and transverse residual stress values for each welding sequence

 DOI : 10.35291/2454-9150.2020.0162

Welding sequence	Maximum longitudinal stress (MPa)		Maximum transverse stress (MPa)		Maximum von misses stress (MPa)
	Tensile	Compressive	Tensile	Compressive	
A	824	818.4	661	702.3	1310.9
B	953.8	840.2	676	702.8	1310.4
C	824	823	664	702	1312.5
D	840.3	519.3	529.8	598.8	1208.5

Maximum tensile and compressive longitudinal and transverse residual stress occurs for welding sequence B. Maximum von misses stress occurs for sequence C whereas for sequence A and B are also closer to maximum. For sequence D, tensile and compressive transverse residual stress and von misses stress are less than other three sequences.

VII. DISTORTIONS

Figure 7.1 and Figure 7.2 illustrates the distortions of the welding structure due to the welding sequences.

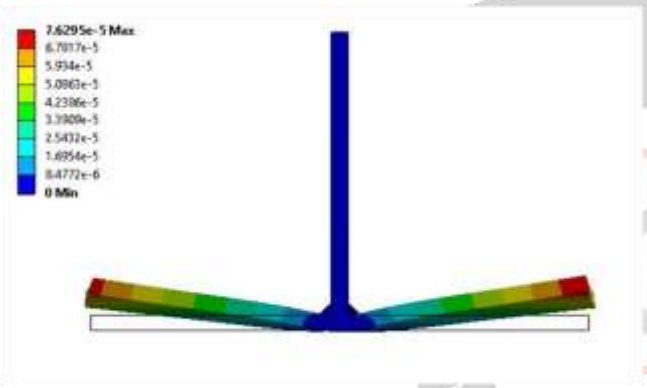

Sequence A

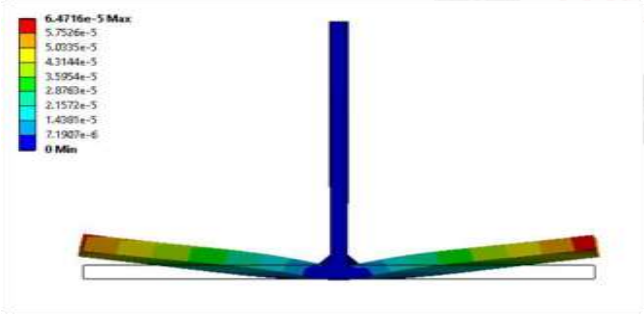

Sequence B

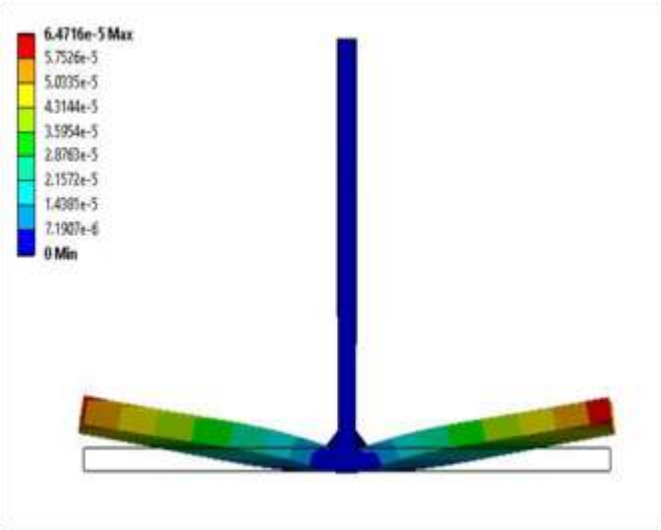

Sequene C

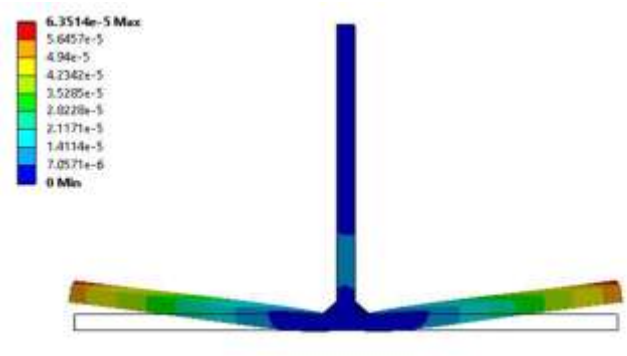

Sequence D

Fig.7.1: Distortion of welding structure due to welding sequences

The initial un-deformed configurations were also shown. From Figure 19, it can be seen the angular distortions occurred in both flanges. It can be further revealed that there was the difference of distortion between the flanges showing that the distortion was unsymmetrical. The maximum value of angular distortion took place on the right flange for all the welding sequences.

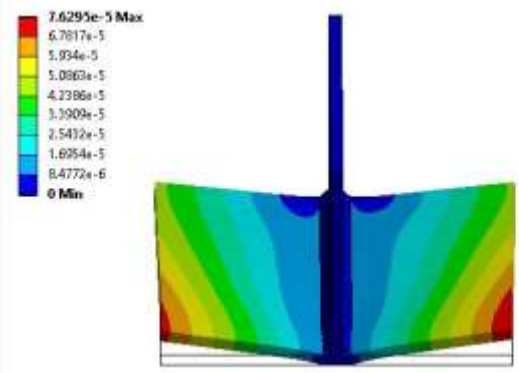

Sequence A

 DOI : 10.35291/2454-9150.2020.0162

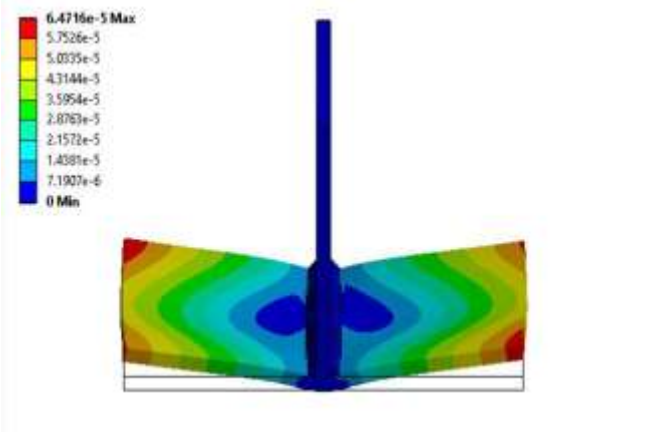

Sequence B

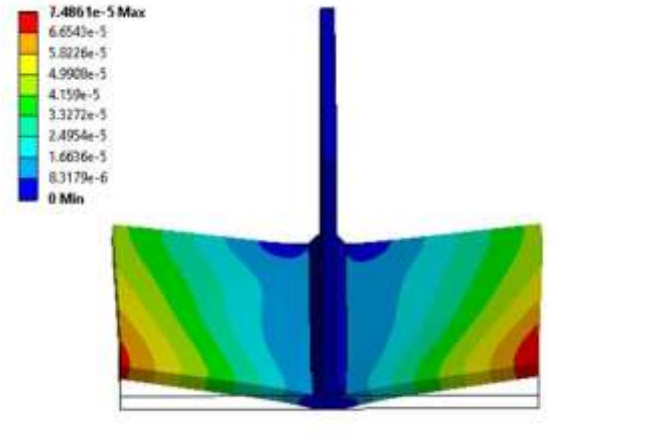

Sequence C

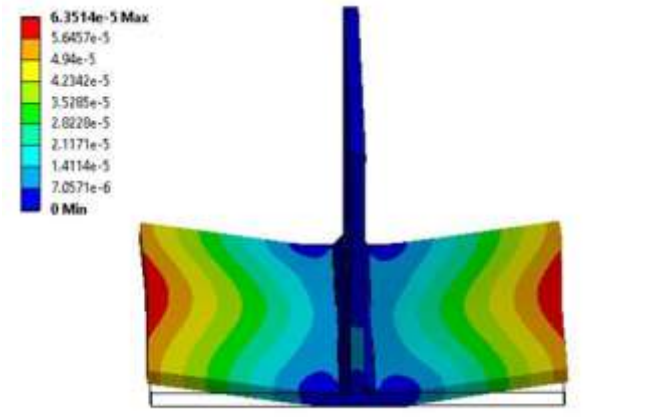

Sequence D

Fig. 7.2: Distortion of welding structure due to welding sequences

From Figure 7.3, it can be seen the distortions occurred in Z-direction for sequence A and sequence C is unsymmetrical. For sequence A, sequence B and sequence C, maximum distortion occurred at front right tip of the plate. Maximum distortion for sequence D occurred at mid-point on right end.

Figure 7.4 shows the displacement in Y-direction for four welding sequence at Z=0.15 m. Vertical displacement for all welding sequences considered shows symmetric behavior about the mid plane. Vertical displacement is high for welding sequence A and sequence C. Sequence D has lowest vertical displacement compared to other welding sequences and it has zero vertical displacement at midpoint.

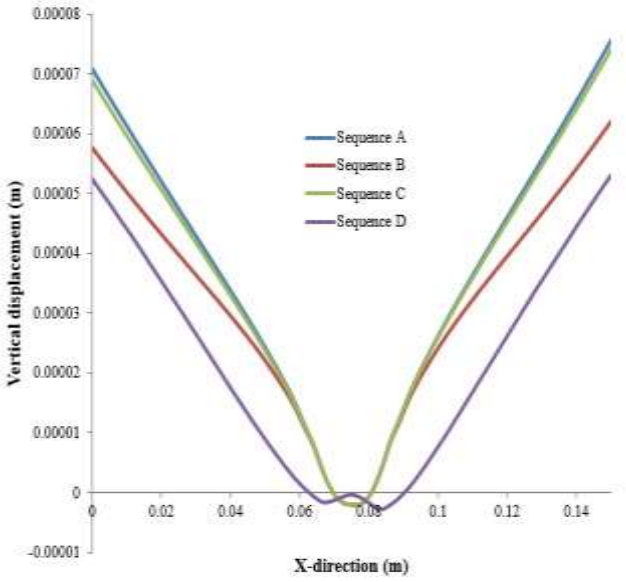

Fig. 7.3: Vertical displacement due to welding sequences

Figure 7.4 shows vertical displacement variation along Z-direction at X=0.15 m and X=0 m. Vertical displacement along Z-direction is unsymmetrical for sequence A and sequence C with maximum vertical displacement at X=0.15 m whereas for sequence B and sequence D shows symmetric behavior. For sequence B, maximum vertical displacement is at the ends and minimum at the center but for sequence D, maximum vertical displacement is at the Centre and minimum at the ends.

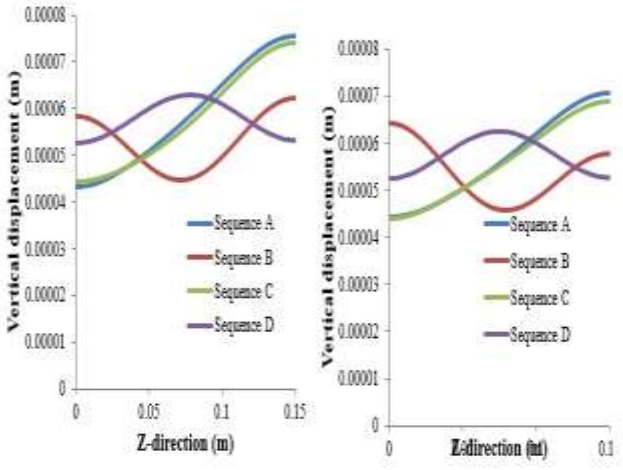

Fig. 7.4: Vertical displacement at X=0.15m and X=0m due to welding sequences

 DOI : 10.35291/2454-9150.2020.0162

VIII. CONCLUSIONS

A finite element model capable of simulating the thermo-mechanical welding process was developed. The finite element simulation was then used to examine the distortion and residual stresses generated during welding for four different welding sequences and their possible effect on the strength of the stiffened plate and distortion was discussed. The following conclusions are drawn from this study.

In case of longitudinal residual stress, peak value occurred for sequence B whereas other three sequences did not show significant variation. . In case of transverse residual stress, it is low for sequence D whereas other three sequences did not show significant variation In case of welding-induced distortion, welding sequence A and sequence C resulted in large distortion and welding sequence D resulted in minimum distortion. Considering both residual stress and distortion as a result of welding, welding sequence D is identified as the preferred welding sequence with the lowest welding-induced residual stress and distortion.

REFERENCES

[1]Effect of welding sequence on residual stress in thin-walled octagonal pipe−plate structure – College of Materials Science and Engineering, Hunan University, Changsha 410082, China; 2. State Key Laboratory of Advanced Design and Manufacture for Vehicle Body, Hunan University, Changsha 410082, China.

[2]Effect of welding Residual stress and Distortion on ship hull structural performance-

By Liam Gannon Submitted in partial fulfillment of the requirements for the degree of Doctor of Philosophy at Dalhousie University Halifax, Nova Scotia.

[3]Numerical Analysis of Effect of Process Parameters on Residual Stress in a Double Side TIG Welded Low Carbon Steel Plate Vishnu V.S1, Nadeera M 2, Joy Varghese V.M3 1, 2 Dept. Of CIM, T.K.M College of engg. / Kerala University, India 3Dept. of ME, SCT College of engg. / Kerala University, India.

[4]Investigation of Arc Welding Variables Influenced by Temperature Cycle Developed in High Carbon Steel Welded Butt Joints and its Effect on Distortion**.** By Jaideep Dutta, Narendranath S Dept.of Mech Engg. NIT, Karnataka, Surathkal, Mangalore-575025, India.

[5] SCHENK T, RICHARDSON I M, KRASKA M, OHNIMUS S. A study on the influence of clamping on welding distortion [J]. Computational Materials Science, 2009, 45: 999−1005. [3] JIANG W C, ZHANG Y C, WOO W C. Using heat sink technology to decrease residual stress in 316L stainless steel welding joint: Finite element simulation [J]. International Journal of Pressure Vessels and Piping.

[6] Rosenthal D. (1941). Mathematical theory of heat distribution during welding and cutting. Welding Journal, 21(5), 220s-234s.

[7] Rosenthal D. (1946), the theory of moving sources of heat and its application to metal treatments. Trans. AIME, 41(11), 849-866.

[8] Friedman E. (1978), Analysis of weld puddle distortion, Welding Journal Research Supplement, pp 161s-166s.

[9] Oddy A. S. et al. (1992). “Transformation plasticity and residual stresses in single-pass repair welds”, ASME Journal Pressure Vessel Technology, 114, 33-38.

 DOI : 10.35291/2454-9150.2020.0162